Distribution of Zinc, Copper, and Iron in the Tailings Dam of an Abandoned Mine in Shimokawa, Hokkaido, Japan

KimLeang Khoeurn[1*], Asuka Sasaki[1], Shingo Tomiyama[2], and Toshifumi Igarashi[2]

[1]Graduate School of Engineering, Hokkaido University, Sapporo, 060-8628, Japan, Tel.: +81-11-706-6311, Fax: +81-11-706-6308; [2]Faculty of Engineering, Hokkaido University, corresponding author's e-mail:khoeurnk@yahoo.com

Abstract This paper addresses the mechanism of acid mine drainage generation in tailings from an abandoned mine site and predicts the evolution of zinc (Zn), copper (Cu), and iron (Fe) concentrations. Batch leaching experiments and sequential extractions were conducted to investigate the leaching behavior of these contaminants from the tailings and to understand their solid-phase partitioning. Acid-base accounting and principal component analysis (PCA) were used to confirm factors affecting Zn, Cu, and Fe leaching and acid formation based on the leaching experiments. There were strong positive correlations between Zn, Fe, or EC and SO_4^{2-}, indicating that pyrite and sphalerite are the major minerals releasing Zn and Fe. This aligns with the PCA results. In the upper part of the tailings, the water-soluble and sulfide fractions of Zn, Cu, and Fe were almost flushed out, whereas they remained high in the deeper tailings. This implies that the tailings will likely continue to release these contaminants (Zn > Cu > Fe) for a long time unless remedial measures are taken.

Keywords: acid mine drainage (AMD), tailings, toxic elements, principal component analysis (PCA)

Introduction

It has been estimated that more than 70% of the materials excavated during mining operations worldwide are wastes (Younger et al. 2002). Mine wastes can generally be classified into two major categories, waste rock and tailings. Tailings are produced when usables ore are separated from unusable materials, before smelting (Zhang et al. 2016).

Many closed mines are located in Hokkaido, Japan, most of which have been continuously generating acid mine drainage (AMD) after their closure (Ito et al. 2010). The primary minerals in the tailings are quartz and pyrite, with secondary minerals such as goethite (Sasaki et al. 2002). The AMD is generated by the weathering of sulfide minerals like pyrite (Younger et al. 2002) when they are exposed to air and water, which has serious negative impacts on the surrounding soil, water resources, and ecosystem (Khan et al. 2008; Lee et al. 2005; Yadav 2010). Some of the metals that dissolve out of the tailings are detrimental to human health when they are ingested through contaminated drinking water and food crops (Duruibe et al. 2007).

AMD generated from tailings dams and drifts at abandoned mine sites are treated before their re-introduction into the environment (Gazea et al. 1995; Gray 1997). The most common and widely used AMD management approach is neutralization by an alkaline reagent (e.g., limestone, quicklime, or sodium hydroxide) to raise the pH and remove most of the metals through precipitation reactions (Matlock et al. 2002; Potgieter-Vermaak et al. 2006). During a short-term period, the neutralization is relatively cheap; however, if the treatment stretches for several decades or centuries, the combined costs of neutralization reagents, facilities, and

sludge disposal become enormous (Ueda and Masuda 2005). In addition, it is difficult to accurately predict when AMD generation will stop.

To select an appropriate remediation strategy, the properties of tailings, metal contents, and their spatial distribution should be clarified (Acosta et al. 2011). The distribution and chemical species of metals in a tailings dam differ, depending on the ore minerals, tailings properties, deposit time, and local climate (Duanmu et al. 2011). Several studies have shown changes in AMD generation rates (Bouzahzah et al. 2014; Greenhill 2000; Hakkou et al. 2008; Lengke et al. 2010; Modabberi et al. 2013; Morin and Hutt 1998; Schafer 2000) and the leaching behaviors of contaminants from mine sites over time (Bogush and Lazareva 2011; Lee et al. 2005; Wang et al. 2017; Zhang et al. 2016). However, the factors and processes controlling AMD generation and distribution of potentially toxic elements in tailings dams are not fully understood. The aim of this study was to characterize the mineralogy and geochemistry of the tailings of a closed mine, to determine the release of acidity and contaminants, such as Zn, Cu, and Fe, from the tailings, and to predict changes in the chemistry of the AMD. The results of this study will be used to design more economical and sustainable mitigation approaches for closed mine sites.

Materials and Methods

Study Site

The study area (Figure 1) is a tailings dam of the Shimokawa mine, which is located about 60 km northeast of Asahikawa city in northern Hokkaido, Japan. The geology within the area of the mine consists of Tertiary strata, pre-Cretaceous black slates, basaltic rocks, and granitic rocks. The Shimokawa group, which is mainly composed of the Tertiary strata, consists of basaltic to andesitic lava flows and volcaniclastic rocks of the middle to late Miocene age (Sugawara 1995). The mineralization occurs in the hanging-wall of a fault zone and is characterized by the coarse-grained nature, existence of spilitic facies with pillow structure, whitish coloration due to abundant carbonate veinlets, and the assemblage of the sulfide minerals (Ishio and Kubota 1969).

Figure 1 will be inserted near here during the printing process

The ore deposit is considered syngenetic (Miyake 1965). The major ore minerals are chalcopyrite, pyrite, pyrrhotite, and sphalerite. The vein minerals were quartz and chlorite (Sato 1967). The ore body and iron sulfide dissemination zones were mined for gold, silver, and Cu, cobalt, Zn, and iron sulfides. Mining started in 1942 and stopped in 1987; the maximum amount of Cu (38,369 t) was produced in 1972. The tailings were deposited in tailings dams. AMD with high concentrations of Zn, Cu, and Fe has been generated at the site since the mine was closed. The bulk of the AMD from the tailings dams and drifts of the mine level has been treated by neutralization for the past 40 years. Representative AMD quality and volume treated in the mine site are shown in Table 1. The concentrations of Zn and Fe exceed Japan's effluent standards, and the Cu concentrations almost exceeds Japan's drinking water standard.

Table 1 will be inserted near here during the printing process

Sampling, and Chemical and Mineralogical Analyses

Figure 2 shows the plain view of the main tailings dam, which is divided into Dams 1, 2 and 3, and a cross-sectional view of one of the dams is shown in Figure 3. These tailings dams are located along a river. The geology of the tailings dam consists of a talus cone, lapilli tuff, terrace deposit, covering soil, and bank (Fig. 3). Dam 1 (about 3.1 ha in area and 10 m deep) was selected in this research because the geology and construction procedures of the three dams were the same. In this site, the average rainfall is 969 mm/year with daily temperature ranging from –9.4 to 20.1 °C. Four boreholes were drilled in the tailings of Dam 1 as shown in Figure 3 (B2, B3, B4, and B5). The depths of boreholes are 10 m for the boreholes B2 and B3, and 6 m for B4 and B5. Total 23 core samples were collected at different depths from B2 to B5. All samples were then dried at the room temperature before analysis.

Figures 2 and 3 will be inserted near here during the printing process

The chemical composition and mineral constituents of the samples were determined using X-ray fluorescence spectrometry (XRF; XEPOS, Rigaku Corp., Japan) and X-ray diffraction spectrometry (XRD; MULTIFLEX, Rigaku Corp., Japan), respectively. Both analyses were done using pressed powders of samples (< 75 μm). Loss on ignition (LOI) was measured by heating 1 g of samples (< 2 mm) inside a furnace for 1 h at 750 °C after oven drying for 24 h at 110 °C.

Batch Leaching Experiments

Batch leaching experiments were carried out to investigate vertical profiles of Zn, Cu, and Fe concentrations leached from different layers. Samples less than 2 mm in diameter were provided for the experiments. Fifteen grams of samples were mixed with 150 mL of deionized water (18 MΩ·cm) in a 250 mL Erlenmeyer flask and the suspensions were mixed using a lateral-reciprocating shaker at a speed of 200 rpm for 6 h at room temperature. After shaking, pH, electrical conductivity (EC), temperature, and oxidation-reduction potential (Eh) of the suspensions were measured, followed by filtration of the leachates through 0.45 μm Millex® filters (Merck Millipore, USA). All filtrates were preserved by acidification (pH < 2) prior to chemical analysis. The concentrations of Zn, Cu, and Fe, and other coexisting elements were analyzed using an inductively-coupled plasma atomic emission spectrometer (ICP-AES; ICPE-9000, Shimadzu Corp., Japan). The standard ICP-AES method has a margin of error of ca. 2−3%, and the detection limits of these elements by the standard ICP-AES range from 0.001 to 0.01 mg/L, for different elements.

Acid-Base Accounting (ABA)

The acid-neutralizing (NP) and acid-generating (AP) potentials of the tailings samples from borehole B3 were measured according to Lawrence and Wang (1997) and Wang et al. (2017). In this measurement, 2 g of pulverized tailings samples were poured into a 250 mL Erlenmeyer flask and approximately 90 mL of distilled water were added. Then, 1 mL of 1 M hydrochloric acid was added to the suspension. After 2 h, another 1 mL of 1 M HCl was added. The suspension was allowed to react at room temperature for 24 h and titrated to pH 8.3 with 1 M sodium hydroxide (NaOH). Equation 1 was used to calculate NP (Lawrence and Wang 1997; Wang et al. 2017). The AP was calculated using the content of sulfide sulfur ($S_{sulfide}$ %; Eq. 2). The $S_{sulfide}$ was determined by leaching experiments with hydrogen peroxide (H_2O_2) and calculated according to Equation 3 (Lengke et al.

2010). In the experiment, 1 g of samples was mixed with 100 mL of 15% H_2O_2 (pH = 7). The solution was kept at room temperature for 48 h and then heated to remove residual H_2O_2. After cooling, the acidity of the suspension was determined by titration until pH 8.3 with 1 M NaOH. The difference between the values of NP and AP is the net acid-neutralizing potential (NNP = NP − AP). If the NNP value is between −20 and 20 kg $CaCO_3$/t, the acid generation is uncertain; if the NNP value is below −20 kg $CaCO_3$/t, acid generation is likely to occur; and if the NNP value is above 20 kg $CaCO_3$/t, it is unlikely to generate any acid (Lengke et al. 2010; Skousen et al. 2002).

$$NP = \frac{50 \times (Xa - Yb)}{c} \quad (1)$$

where, NP (kg $CaCO_3$/t), X: volume of HCl (mL), Y: volume of NaOH (mL), a: normality of HCl (mol/L), b: normality of NaOH (mol/L), and c: mass of sample (g).

$$AP = 31.25 \times S_{sulfide} \quad (2)$$

$$S_{sulfide} = 1.6 \times V \quad (3)$$

where, AP (kg $CaCO_3$)/t and V: Volume of NaOH (mL)

Sequential Extraction

Selective sequential chemical extractions are often used to determine the distribution of Zn, Cu, and Fe with different sorptive phases and their mobilization in soils and mine wastes (Dold and Fontboté 2001). This method operationally partitions Zn, Cu, and Fe into six fractions: (1) water-soluble, (2) exchangeable, (3) carbonate, (4) poorly crystalline, (5) crystalline, and (6) sulfide/organic matter fraction (Table 2). The tailings samples from borehole B3 at different depths were used for sequential extraction and it was done in duplicate. One gram of samples was mixed with an extractant (Table 2) in a 50 mL centrifuge tube. The solid-liquid separation was achieved by centrifugation at 4,000 rpm for 45 min. The supernatant was then separated by a pipette and placed in a clean 50 mL volumetric flask. The residue was washed with 8 mL of deionized water before the next step was carried out. The mixture of the supernatant and washed water was provided for analysis of Zn, Cu, and Fe using ICP-AES. For the residue, the extractant was changed to proceed to the next fraction.

Table 2 will be inserted near here during the printing process

Statistical Analysis Using Data of Batch Leaching Experiments

The batch leaching experimental data were analysed using principal component analysis (PCA) by OriginPro 2017 to understand the correlations between the different variables and to evaluate major components representing the leaching of Zn, Cu, and Fe from the tailings. The principal components were simplified by varimax rotation to increase the participation in the variables with higher contribution and reduce the participation in the other variables. Fourteen variables were used in the PCA.

Results and Discussion

Characterization of Core Samples

The geology of B2 from the ground surface consists of oxidized tailings, tailings, terrace deposit, and lapilli tuff; that of B3 consists of oxidized tailings, tailings, and lapilli tuff; that of B4 consists of soil covering, tailings, and lapilli tuff; and that of B5 consists of tailings and lapilli tuff. The chemical compositions of samples from each borehole are listed in Supplemental Table 1. Among all samples, the tailings, including oxidized tailings, contained greater levels of Zn (317−19,400 mg/kg), Cu (271−4,190 mg/kg), and Pb (18–48 mg/kg) than the lapilli tuff, covering soil, and terrace sediment samples. In the oxidized tailings, the contents of these elements (317−362 mg/kg for Zn, 271−464 mg/kg for Cu, and 25−34 mg/kg for Pb) were generally less than those of the deeper, unweathered tailings (3,800−19,400 mg/kg for Zn, 1,350−4,190 mg/kg for Cu, and 10−55 mg/kg for Pb). Similarly, the content of Fe_2O_3 was lower in the oxidized tailings samples (2.9−5.5 wt%) than in the deeper tailings samples (10−20 wt%). Sulfur content was also less in the oxidized tailings (0.3−0.6 wt%) than in the deeper, unweathered tailings (2.5−5.5 wt%). These results indicate that Zn, Cu, Fe, and S had leached out of the weathered tailings in the top 0–0.4 m of the tailings during the past 40 years.

The XRD analytical results (Supplemental Table 2) showed that the major minerals in the tailings were quartz and albite while the pyrite and sphalerite were detected as trace components. Nantokite and chlorite were also detected in the tailings samples. Iron-bearing minerals like goethite (FeOOH), schwertmannite, and ferrihydrite probably existed in the tailings but were not detected by XRD even though the Fe contents (3−20.6 wt%) were quite substantial. This may be due to their content being less than the detection limits or their amorphous form (Carlson and Schwertmann 1981; Herbert 1994). The soil, terrace deposit, and lapilli tuff contained quartz, albite, and anorthite, but no sulfide minerals were detected. The presence of pyrite in the tailings implies that weathering will continue to release acid water containing Zn, Cu, and Fe, although no Zn-, Cu-, or Fe-bearing minerals were detected.

Batch Leaching Experiments

Figures 4 to 6 illustrate the vertical distribution of pH, Eh, and concentrations of Zn, Cu, and Fe in batch leaching experiments, respectively, at boreholes B2, B3, B4, and B5. The geology of each borehole is described on the right side of each graph. The oxidized tailings are shown as light gray, the unweathered tailings as dark gray, the soil and bank is reddish-brown, the terrace deposit is blue, and lapilli tuff is green.

Figures 4, 5, and 6 will be inserted near here during the printing process

The pH values of the samples were 3.5–6 at B2, 4–7 at B3, 3–5 at B4, and 3–8 at B5. The higher pH values were found in the terrace deposit, lapilli tuff, and covering soil whereas the lower pH values were found in the tailings samples. These results showed that the tailings had an acidic pH, and are the main source of the acid water. The Eh was positive, irrespective of samples, ranging from 360–590 mV. These results were similar to those of Adnani et al. (2016).

The leached concentrations of Zn, Cu, and Fe were higher in the tailings samples (Zn ranging from 0.3 to

400 mg/L, Cu ranging from 0.2 to 300 mg/L, and Fe ranging from 0.5 to 50 mg/L) than in the other layers and in the order: Zn > Cu > Fe. The distribution of SO_4^{2-} was similar to those of Zn, Cu, and Fe. Focusing on only the tailings samples, the concentrations of Zn, Cu, Fe, and SO_4^{2-} were lower in the upper oxidized tailings. In fact, it appears that only the upper tailings have weathered; most parent sulfide minerals were transformed to secondary minerals, such as oxides, sulfates, and exchangeable fractions, and then flushed out, resulting in lower leaching concentrations. The leaching concentrations of Zn, Cu, Fe, and SO_4^{2-} in the deeper tailings remained higher (Fig. 6). However, the leaching concentrations of Zn, Cu, Fe, and SO_4^{2-} at the bottom part of the tailings were less than those in the middle part of the tailings. This means that Zn, Cu, Fe, and SO_4^{2-} were flushed out by greater groundwater flow near the weathered lapilli tuff, which has a higher hydraulic conductivity (10^{-5} m/s) than the tailings (10^{-7} m/s). Lead was not detected in the leachate of the batch leaching experiments although the tailings contained Pb.

The lower pH values in the batch leaching experiments likely resulted from pyrite oxidation, leading to higher Zn, Cu, Fe, and SO_4^{2-} concentrations (Figs. 4 and 6). Similar results were described by Todd et al. (2003). It was also found that the acid produced by pyrite oxidation enhanced the mobility of Zn, Cu, and Fe, dissolution of solids, and SO_4^{2-} (Devasahayam 2007; Dold and Fontboté 2001).

Acid-Base Accounting (ABA)

Table 3 summarizes the results of the modified ABA static tests of the tailings samples from borehole B3. All tailings samples had low NP values, ranging from −8.75 to 18.75 kg $CaCO_3$/t, whereas the AP values were between 20 and 70 kg $CaCO_3$/t, which corresponds to negative NNP values, ranging from −73.7 to −23.7 kg $CaCO_3$/t. The NNP values clearly indicate that the tailings are acid-generating, which is consistent with the XRD results showing the existence of pyrite and the low pH values of the leaching experiments.

Table 3 will be inserted near here during the printing process

Solid-Phase Partitioning of Zn, Cu, and Fe

Results of the sequential extraction of tailings samples from borehole B3 are shown in Figures 7 (a), (b), and (c) for Zn, Cu, and Fe, respectively. The water-soluble fraction of Zn and Cu were greater in the middle part of the tailings, and lower at the surface and bottom of the tailings (Figs. 7(a), and (b)). The water-soluble fraction of Fe was negligible irrespective with depth (Fig. 7(c)). These results reflect that the water-soluble fractions of these elements were almost flushed out from the oxidized tailings and the bottom of the tailings. The amounts of Zn, Cu, and Fe in the water-soluble fraction were likely related to the degree of oxidation.

Figure 7 will be inserted near here during the printing process

The NH_4-acetate extractant is used to determine the exchangeable elements at pH 4 to 5, and calcite is also dissolved by this extractant (Dold and Fontboté 2001). The exchangeable and carbonate fractions are separated by using the same extractant (NH_4-acetate) at pH 7 and 5, respectively (Bogush and Lazareva 2011). The exchangeable fractions of Fe was negligible in all of the tailings samples while those of Zn and Cu were <0.3 and 7%, respectively. The Fe carbonate fraction was negligible in the tailings whereas those of Zn and Cu in the surface tailings were 2 and 4%, respectively, much higher than deeper in the tailings. This can be explained by

the addition of calcium carbonate as a neutralizer in the shallower part of the tailings dams. It is inferred that AMD was prevented for a while by the addition of the neutralizer when the tailings were being deposited.

The application of 0.2 M HN_4-oxalate at pH 3 extracted secondary ferric phases, such as schwertmnnite and jarosite. The Fe content of this poorly crystalline fraction ranged from 12 to 23%, with less found at the surface of the tailings. On the other hand, the levels of Zn and Cu associated with this fraction were higher in the oxidized tailings (8% for Zn and 13% for Cu) than in the deeper tailings (1.4−4% for Zn and 2−10% for Cu). These results suggest that the secondary Fe-bearing minerals formed at the surface of the tailings co-precipitate or adsorb Zn and Cu.

Crystalline Zn, Cu, and Fe were relatively abundant in the oxidized tailings (47% for Zn, 33% for Cu, and 45% for Fe) and decreased with depth (0.3−2.5% for Zn, 0.04−0.4% for Cu, and 9−22% for Fe). The high contents of these elements suggest that ferrihydrite or goethite likely precipitated in the upper part of the tailings, and that Zn and Cu may be absorbed or incorporated into the structure of the Fe(III) oxyhydroxide minerals. Crystalline and poorly crystalline Fe compounds in the weathered tailings can act as a sink of trace elements (Cu, Pb, Se, and Zn) through adsorption, substitution, or co-precipitation (Khorasanipour et al. 2011; McGregor and Blowes 2002). Thus, these elements in crystalline and poorly crystalline phases are considered stable; however, these elements can be slowly released over time (Fadiran et al. 2014).

The highest amounts of Zn, Cu, and Fe occurred in the sulfide fraction and generally increased with depth. Sulfur content was also depleted in the surface tailings (Supplemental Table 1). This indicates that the weathering of sulfide minerals has generally proceeded from the surface during the past 40 years.

Zn, Cu, and Fe contained in sulfides are transformed into water-soluble/exchangeable fractions by oxidation, and then into crystalline and poorly crystalline mineral forms; thus, the tailings are likely to continue to release Zn, Cu, and Fe. The upper tailings have been oxidized because of the abundance of oxygen and water, and the soluble Zn, Cu, and Fe have been almost leached out from these tailings. However, the deeper tailings have not yet oxidized because of the lower concentrations of electron donor. The contaminants in the middle parts of the tailings could be mobilized when they contact air and water.

Statistical Analysis of Obtained Data

Multivariate statistical analysis and PCA were used to reduce the number of variables to confirm the most representative variables and to support the interpretation of the geochemical data from the tailings samples. PCA has been used for multivariate analysis of contaminant leaching from soil (Li et al. 2015) and to predict the geochemical hazards of coal mine tailings (Park et al. 2017). Table 4 lists the correlation coefficients of the results of the leaching experiments. Strong positive correlations (correlation coefficient > 0.8) were found for Fe-SO_4^{2-}, Zn-SO_4^{2-}, EC-SO_4^{2-}, Ca-EC, K-Na, and pH-Eh. The strong positive correlations of Fe-SO_4^{2-}, Zn-SO_4^{2-}, and EC-SO_4^{2-} reflect the fact that pyrite and sphalerite are likely the major minerals releasing Fe and Zn from the tailings. As expected, a negative correlation was observed between Fe-pH and SO_4^{2-}-pH (i.e., correlation coefficient < −0.6) (Table 4), so a lower pH (higher acidity) was related to higher concentrations of Fe and SO_4^{2-}.

Table 4 will be inserted near here during the printing process

Table 5 shows the PCA results of the leaching experiments. The first three components accounted for 79%

of the total variation. The loadings of the first component were larger for Zn, Cu, Fe, SO_4^{2-}, pH, EC, and Eh, which accounted for 46% of the total variance. This simply reflects the fact that the sulfide minerals (e.g. pyrite, sphalerite, and chalcopyrite) produce Zn, Cu, Fe, and SO_4^{2-}. These minerals also contribute to the contamination from the tailings. The loadings of the second component, which was 19%, were attributed to K, Na, and Si, reflecting the fact that minerals like feldspar influenced K, Na, and Si leaching concentrations. However, the third component accounted for 14% of total variance, which was dominated by Ca. This likely reflects the addition of a neutralizer during tailings deposition, as pointed out by the sequential extraction results.

Table 5 will be inserted near here during the printing process

Figure 8 shows a dendrogram of cluster analysis of leaching experiments of the tailings samples. This figure clearly reveals two clusters: (1) the middle part of the tailings, which produce acidic water containing Zn, Cu, and Fe; and (2) the tailings near the lapilli tuff and immediately below the weathered tailings, which produce a higher pH.

Figure 8 will be inserted near here during the printing process

Conclusion

The tailings dams of the Shimokawa mine were characterized by leaching experiments, ABA, and sequential extraction. Pyrite was the main factor controlling AMD formation and mobilization of Zn, Cu, Fe, and SO_4^{2-} in the tailings. The NNP values of the tailings were less than –20 kg $CaCO_3$/t, indicating that the tailings still have acid-generating potential. Although the tailings were disposed of 40 years ago, the tailings will likely continue to produce AMD containing Zn, Cu, and Fe for a long period of time unless remedial measures are taken.

The leaching concentrations, total contents, and sulfide fractions of Zn, Cu, and Fe were higher in the samples in the deeper part of the tailings than in the oxidized tailings, lapilli tuff, covering soil, and terrace deposit. The Zn, Cu, and Fe in the tailings were mainly bound to the sulfide and water-soluble fractions. However, weathering transforms these elements from sulfide to exchangeable/water-soluble and poorly crystalline and crystalline forms. In addition, some of Zn and Cu may be adsorbed onto or incorporated into the Fe(III) oxyhydroxide minerals.

Acknowledgments The authors gratefully appreciate EcoManagement Corporation for the assistance during the field sampling and for providing us with the geological data of the study site. The authors wish to thank the anonymous reviewers for their valuable input to this paper. The authors would like also to thank the Editor-in-Chief and Associate Editor for their helpful comments and reviews of the English language in this paper.

References

Acosta JA, Jansen B, Kalbitz K, Faz A, Martinez-Martinez S (2011) Salinity increases mobility of heavy metals in soils. Chemosphere 85: 1318 - 1324

Adnani MEl, Plante B, Benzaazoua M, Hakkou R, Bouzahzah H (2016) Tailing weathering and arsenic mobility

281 at the abandoned Zgounder Silver Mine, Morocco. Mine Water Environ 35: 508-524
282 Bogush AA, Lazareva EV (2011) Behavior of heavy metals in sulfide mine tailings and bottom sediment (Salair,
283 Kemeovo region, Russia). Environ Earth Sci 64: 1293-1302
284 Bouzahzah H, Benzaazoua M, Bussiere B, Plante B (2014) Prediction of acid mine drainage: Importance of
285 mineralogy and the test protocols for static and kinetic tests. Mine Water Environ 33: 54-65
286 Carlson L, Schwertmann U (1981) Natural ferrihydrites in surface deposit from Finland and their association
287 with silica. Geochim. Cosmochim. Acta 45: 421-429
288 Devasahayam S (2007) Application of particle size distribution analysis in evaluating the weathering in coal
289 mine rejects and tailings. Fuel Process Technol 88: 295-301
290 Dold B (2003) Speciation of the most soluble phases in a sequential extraction procedure adapted for
291 geochemical studies of copper sulfide mine waste. J Geochem Explor 80: 55- 68
292 Dold B, Fontbote L (2001) Element cycling and secondary mineralogy in porphyry copper tailings as a function
293 of climate, primary mineralogy, and mineral processing. J Geochem Explor 74: 3-55
294 Duanmu HS, Kang XJ, Li WS (2011) A study of heavy metal geochemistry behavior during oxidation in the
295 mine tailings. Acta Mineral Sinica 31: 153 - 159
296 Duruibe JO, Ogwuegbu MOC, Egwurugwu JN (2007) Heavy metal pollution and human biotoxic effects. Int J
297 Phys Sci 2 (5): 112-118
298 Fadiran AO, Tiruneh AT, Mtshali JS (2014) Assessment of mobility and bioavailability of heavy metals in
299 sewage sludge from Swaziland through speciation analysis. Am J Environ Protect 3: 198 - 208
300 Gazea B, Adam K, Kontopoulos A (1995) A review of passive system for the treatment of acid mine drainage.
301 Miner. Eng. 9(1): 23-42
302 Gray NF (1997) Environmental impact and remediation of acid mine drainage: A management problem. Environ
303 Geol. 30(1): 62-71
304 Greenhill PG (2000) AMIRA international: AMD research through industry collaboration. Proc, 5th International
305 Conference on Acid Rock Drainage (ICARD), vol 1, pp 13-19
306 Hakkou R, Benzaazoua M, Bussière B (2008) Acid mine drainage at the abandoned Kettara mine (Morocco): 1.
307 environmental characterization. Mine Water Environ 27: 145–159
308 Hall GEM, Vaive JE, Beer R, Hoashi M (1996) Selective leaches revisited, with emphasis on the amorphous Fe
309 oxyhydroxide phase extraction. J Geochem Explor 56: 59 - 78.
310 Herbert Jr RB (1997) Properties of goethite and jarosite precipitated from acid groundwater, Dalarna, Sweden.
311 Clays Clay Miner 45(2): 261-273.
312 Ishio H, Kubota Y (1969) On the geology and ore deposits of the Shimokwa Mine, especially of the Nakanosawa
313 area. J Soc Min Geol Jpn 19: 160-169 (in Japanese)
314 Ito F, Nomura T, Katahira K, Kitagawa M, Moriwaki H (2010) Influence of pollution from abandoned sulfur
315 mines on riverine environment: Water quality and microbial habitats in Dodo river system. Seikatsu Eisei
316 54: 321-329. (In Japanese with English abstract)
317 Khan S, Cao Q, Zheng YM, Huang YZ, Zhu YG (2008) Health risk of heavy metals in contaminated soils and
318 food crops irrigated with wastewater in Beijing, China. Environ Pollut 152: 686-692.

Khorasanipour M, Tangestani MH, Naseh R, Hajmohammadi H (2011) Hydrochemistry mineralogy and chemical fractionation of mine and processing wastes associated with porphyry copper mines: a case study from the Sarcheshmeh mine, SE Iran. Appl Geochem 26: 714-730

Lawrence KA, Wang Y (1997) Determination of neutralization potential in the prediction of acid rock drainage. Proc, 4th ICARD, Vancouver, pp 451-464

Lee JS, Chon HT, Kim KW (2005) Human risk assessment of As, Cd, Cu and Zn in the abandoned metal mine site. Environ Geochem Health 27: 185-191

Lengke MF, Davis A, Bucknam C (2010) Improving management of potentially acid generating waste rock. Mine Water Environ 29: 29-44

Li J, Jia C, Lu Y, Tang S, Shim H (2015) Multivariate analysis of heavy metal leaching from urban soils following simulated acid rain. Microchem. J. 122: 89-95

Matlock MM, Howerton BS, Atwood DA (2002) Chemical precipitation of heavy metals from acid mine drainage. Water Res. 36: 4757-4764.

McGregor RG, Blowes DW (2002) The physical, chemical and mineralogical properties of three cemented layers within sulfide-bearing mine tailings. J Geochem Explor 76: 195-207

Miyake T (1965) On genesis of Japanese ‘Kieslager’ deposits with special reference to that of the Shimokawa Mine. J Balneol Soc Jpn 15: 1-11 (in Japanese)

Modabberi S, Alizadgegan A, Mirnejad H, Esmaeilzadeh E (2013) Prediction of AMD generation potential in mining waste piles in the Sarcheshmeh porphyry copper deposit, Iran. Environ Monit Assess 185: 9077-9087

Morin AK, Hutt NM (1998) Kinetic tests and risk assessment for ARD. Proc, 5th Annual BC metal leaching and ARD workshop, Vancouver, available at: http://www.mdag.com/

Park JH, Edraki M, Baumgartl T (2017) A practical testing approach to predict the geochemical hazards of in-pit coal mine tailings and rejects. Catena148: 3-10

Potgieter-Vermaak SS, Potgieter JH, Monama P, Grieken RV (2006) Comparison of limestone, dolomite and fly ash as pre-treatment agents for acid mine drainage. Miner Eng 19: 454-46

Sasaki K, Haga T, Hirajima T, Kurosawa K, Tsunekawa M (2002) Distribution and transition of heavy metals in mine tailings dumps. Mater Trans 43: 2778-2783

Sato S (1967) Shimokawa Mine. J Min Metallurg I Jpn 83: 1723-1728

Schafer WM (2000) Use of the net acid generation pH test for assessing risk of acid generation. Proc, 5th ICARD, vol 1, pp 613 – 618

Skousen J, Simmons J, McDonald LM, Ziemkiewicz P (2002) Acid–base accounting to predict post-mining drainage quality on surface mines. J Environ Qual 31: 2034–2044

Sugawara M, Yamahara I, Okamura S, Nishido H (1995) Miocene volcanism and primitive basalt from Shimokawa district, north Hokkaido, Japan: constraints on Miocene tectonics from petrogenesis of primary magma, Mem Geol Soc Japan 44: 23-37 (in Japanese)

Todd EC, Sherman DM, Purton JA (2003) Surface oxidation of pyrite under ambient atmospheric and aqueous (pH = 2 to 10) conditions: electronic structure and mineralogy from x-ray absorption spectroscopy.

Geochim Cosmochim Acta 67: 881-893
Ueda H, Masuda N (2005) An analysis on mine drainage treatment cost and the technical development to prevent mine pollution. Shigen-to-Sozai 121: 323-329. (In Japanese with English abstract)
Wang L, Li Y, Wang H, Cui X, Wang X, Lu A, Wang X, Wang C, Gan D (2017) Weathering behavior and metal mobility of tailings under an extremely arid climate at Jinchuan Cu-Ni sulfide deposit, Western China. J Geochem Explor 173: 1-12
Yadav SK (2010) Heavy metal toxicity in plants: An overview on the role of glutathione and phytochelatins in heavy metal stress tolerance of plants. S Afr J Bot 76: 167-179
Younger PL, Banwart SA, Hedin RS (2002) Mine Water Hydrology, Pollution, Remediation. Kluwer Academic Publ, London
Zhang W, Alakangas L, Wei Z, Long J (2016) Geochemical evaluation of heavy metal migration in Pb-Zn tailings covered by different topsoils, J Geochem Explor 165: 134-142

Figure captions

Fig. 1 Location of the Shimokawa mine
Fig. 2 Plain view of the tailings dams in the study site
Fig. 3 Cross-sectional view of line A-A' in Fig. 2
Fig. 4 Vertical profiles of pH at B2 (a), B3 (b), B4 (c), and at B5 (d) in batch leaching experiments
Fig. 5 Vertical profiles of Eh at B2 (a), B3 (b), B4 (c), and at B5 (d) in batch leaching experiments
Fig. 6 Vertical profiles of Zn, Cu, Fe, and sulfate concentrations at B2 (a), B3 (b), B4 (c), and B5 (d) in batch leaching experiments
Fig. 7 Results of seqential extraction of Zn, Cu, and Fe in the tailings samples from borehole B3: Zn (a), Cu (b), and Fe (c)
Fig. 8 Dendrogram of results of leaching experiments of the tailings samples

Table 1 The quality of AMD in 2002 and 2010

Year	pH	Heavy metal concentrations			Treated quantity
		Zn (mg/L)	Cu (mg/L)	Fe (mg/L)	(m^3/min)
2002	3.33	5.5	0.89	55.4	0.068
2010	3.52	8.6	0.62	71.4	0.041

Table 2 Summary of sequential extraction procedure for heavy metals from tailings

Extraction step	Procedure	Preferentially dissolved minerals	References
1	1 g tailings, 50 mL deionized water, shaking for 1 h at room temperature (RT)	Water soluble fraction (e.g., gypsum)	Dold and Fontboté (2001)
2	1 M $C_2H_7NO_2$ at pH 7, shaking for 2 h at RT	Exchangeable fraction	Bogush and Lazareva (2011)
3	1 M $C_2H_7NO_2$ at pH 5, pH adjusted with acetic acid, shaking for 2 h at RT	Carbonate fraction (e.g., dolomite, calcite)	Dold and Fontboté (2001)
4	0.2 M $C_2H_8N_2O_4$ at pH 3, pH adjusted with oxalic acid, shaking for 1 h in darkness (using aluminum foil)	Poorly crystalline fraction (e.g., schwertmannite, amorphous ferrihydrite, manganese oxides)	Dold and Fontboté (2001)
5	0.2 M $C_2H_8N_2O_4$ at pH 3, pH adjusted with oxalic acid, heating in water bath at 80 °C for 2 h	Crystalline fraction (e.g., goethite, hematite, magnetite, jarosite, higher order ferrihydrite)	Dold and Fontboté (2001)
6	750 mg of $KClO_3$ and 15 mL 12 HCl, added 10 mL of 4 M HNO_3, water bath at 90 °C for 20 min	Sulfide/organic fraction	Hall et al. (1996); Dold (2003)

Table 3 Acid-base accounting of the tailings samples from borehole B3

Depth (m)	kg $CaCO_3$/t		
	AP	NP	NNP
0.2-0.4	20.0	-3.80	-23.7
2-2.2	60.0	-2.50	-62.5
3-3.2	65.0	-8.80	-73.7
5-5.2	70.0	18.80	-51.3
7-7.2	62.5	6.24	-56.3
8-8.2	55.0	5.93	-49.1

Table 4 Correlation coefficients of analyzed items (Significant correlations are marked in bold)

Variables	Al	Ca	Cd	Cu	Fe	K	Na	Zn	Si	Cl^-	SO_4^{2-}	pH	EC	Eh
Al	1.000													
Ca	-0.120	1.000												
Cd	**0.564**	-0.041	1.000											
Cu	**0.752**	0.249	0.417	1.000										
Fe	**0.657**	0.431	**0.572**	**0.755**	1.000									
K	-0.370	-0.145	-0.213	-0.352	-0.172	1.000								
Na	-0.435	0.032	-0.430	-0.376	-0.292	**0.827**	1.000							
Zn	0.310	0.494	**0.560**	0.413	**0.772**	-0.227	-0.227	1.000						
Si	-0.182	0.161	0.063	-0.090	0.169	**0.745**	0.414	0.132	1.000					
Cl^-	-0.148	0.299	0.046	0.058	0.163	-0.281	-0.042	**0.624**	-0.088	1.000				
SO_4^{2-}	0.376	0.780	0.395	**0.639**	**0.831**	-0.189	-0.173	**0.814**	0.275	0.393	1.000			
pH	**-0.544**	-0.161	**-0.588**	-0.497	**-0.679**	0.062	0.057	**-0.740**	-0.185	-0.372	**-0.590**	1.000		
EC	0.236	**0.840**	0.305	**0.507**	**0.746**	-0.126	-0.094	**0.786**	0.346	0.420	**0.983**	**-0.523**	1.000	
Eh	**0.688**	0.069	**0.671**	**0.559**	**0.679**	-0.091	-0.092	**0.677**	0.125	0.260	**0.554**	**-0.970**	0.468	1.000

Table 5 Results of the principal component analysis of leaching experiments

Parameters	PC1	PC2	PC3
Al	0.252	-0.320	0.288
Ca	0.193	0.292	**-0.425**
Cd	0.257	-0.169	0.264
Cu	**0.294**	-0.170	0.064
Fe	**0.360**	0.016	0.080
K	-0.130	**0.452**	**0.402**
Na	-0.137	**0.450**	0.205
Zn	**0.346**	0.113	-0.109
Si	0.041	**0.466**	0.286
Cl^-	0.155	0.116	-0.351
SO_4^{2-}	**0.354**	0.186	-0.164
pH	**-0.320**	-0.046	-0.249
EC	**0.325**	0.259	-0.213
Eh	**0.319**	-0.028	0.319
Eigenvalues	6.422	2.688	1.949
Percentage of variance (%)	46	19	14
Cumulative (%)	46	65	79

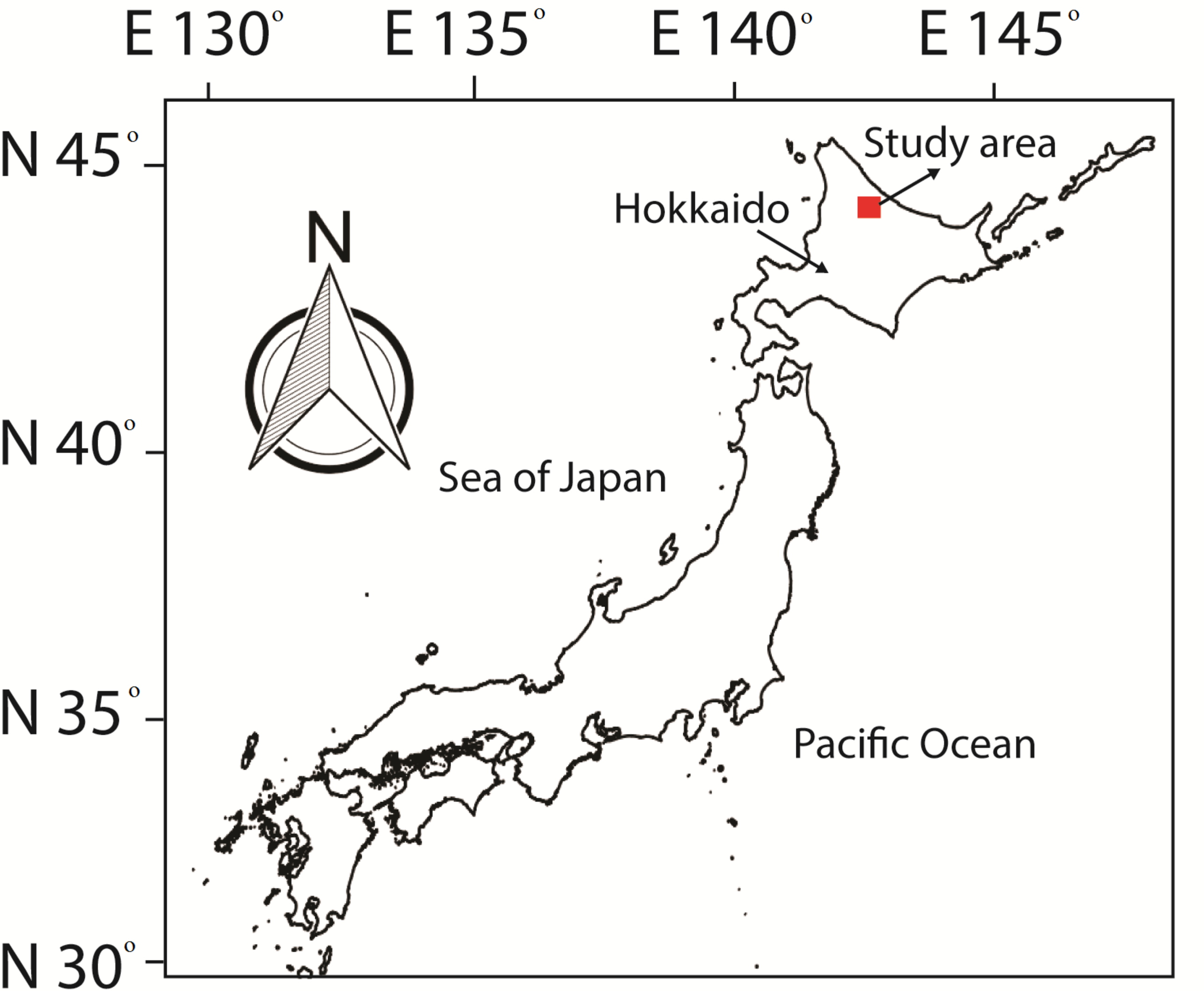
E 130°
E 135°
E 140°
E 145°
N 45°
N 40°
N 35°
N 30°
N
Study area
Hokkaido
Sea of Japan
Pacific Ocean

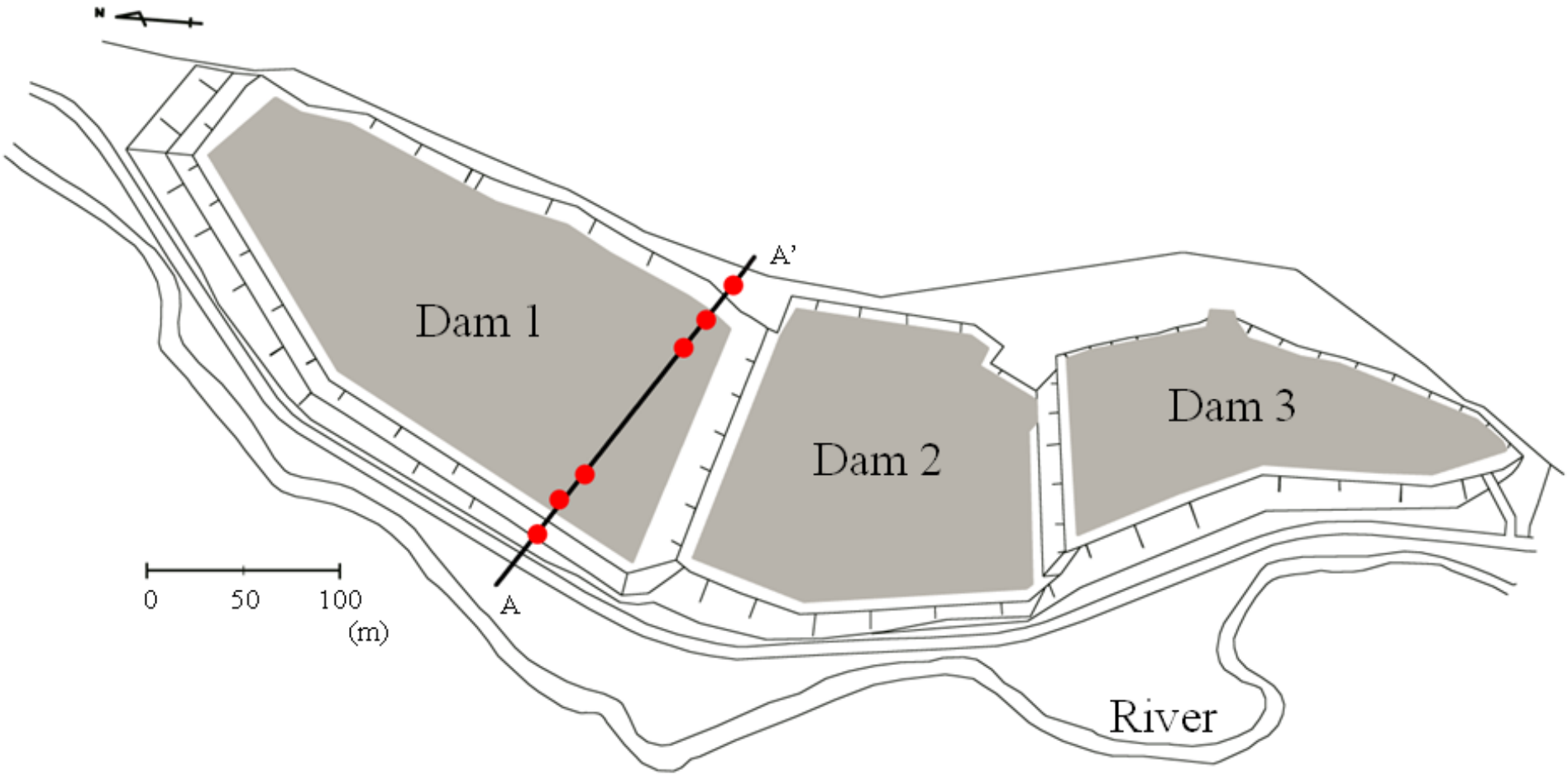
N
Dam 1
Dam 2
Dam 3
A'
A
0
50
100
(m)
River

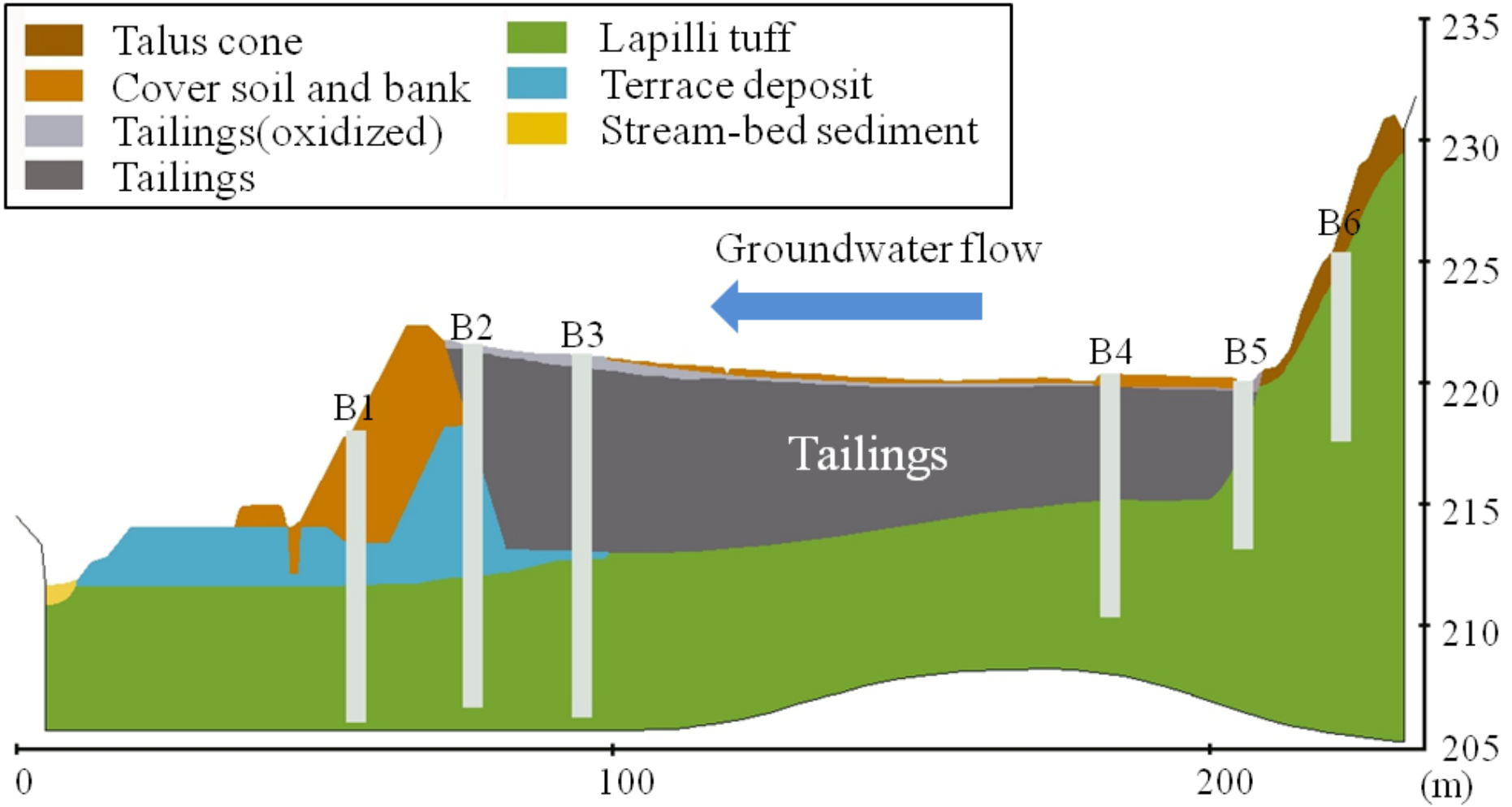
Talus cone
Cover soil and bank
Tailings(oxidized)
Tailings
Lapilli tuff
Terrace deposit
Stream-bed sediment
Groundwater flow
B1
B2
B3
B4
B5
B6
Tailings
235
230
225
220
215
210
205
0
100
200
(m)

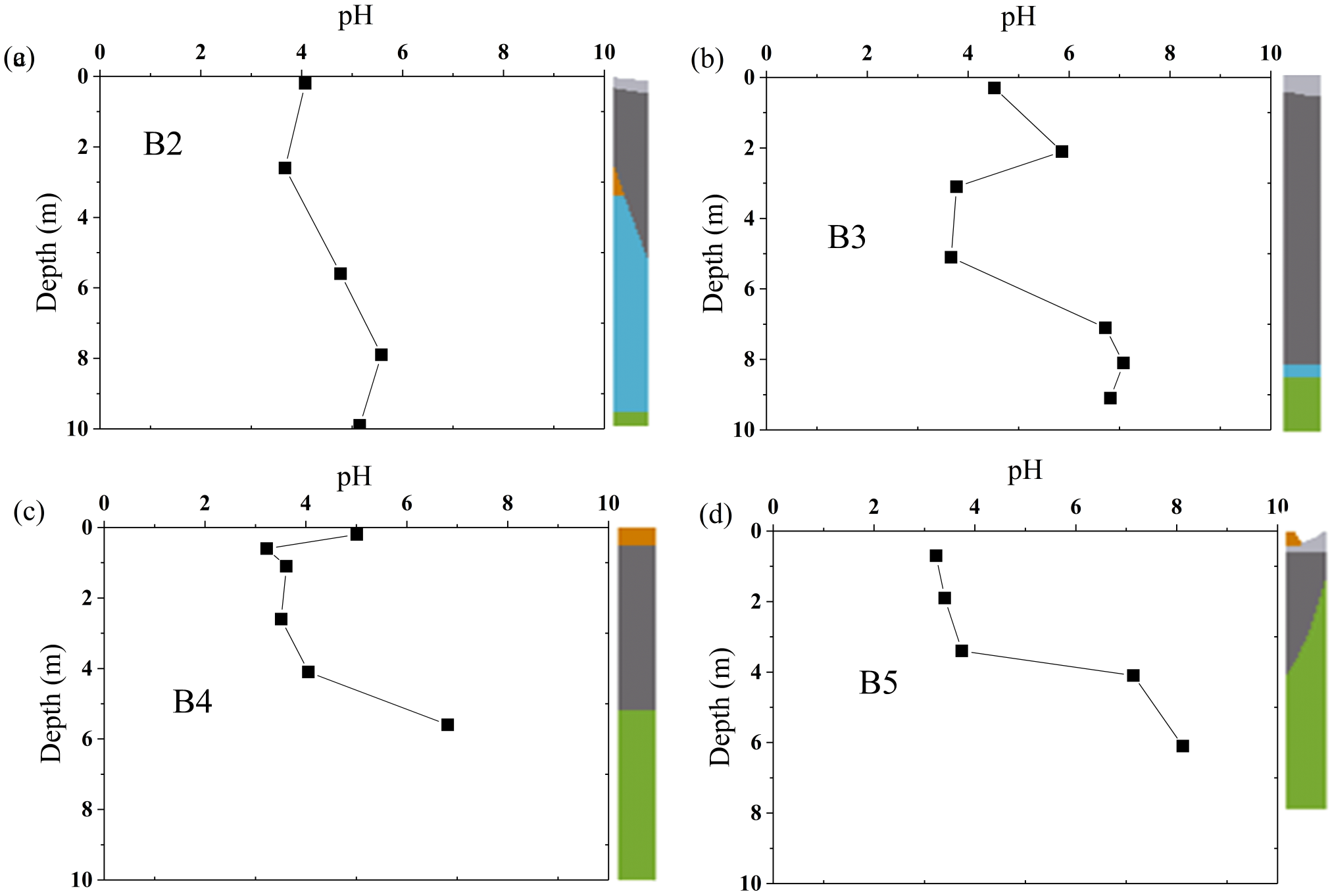
(a)
pH
0
2
4
6
8
10
Depth (m)
B2
(b)
B3
(c)
B4
(d)
B5

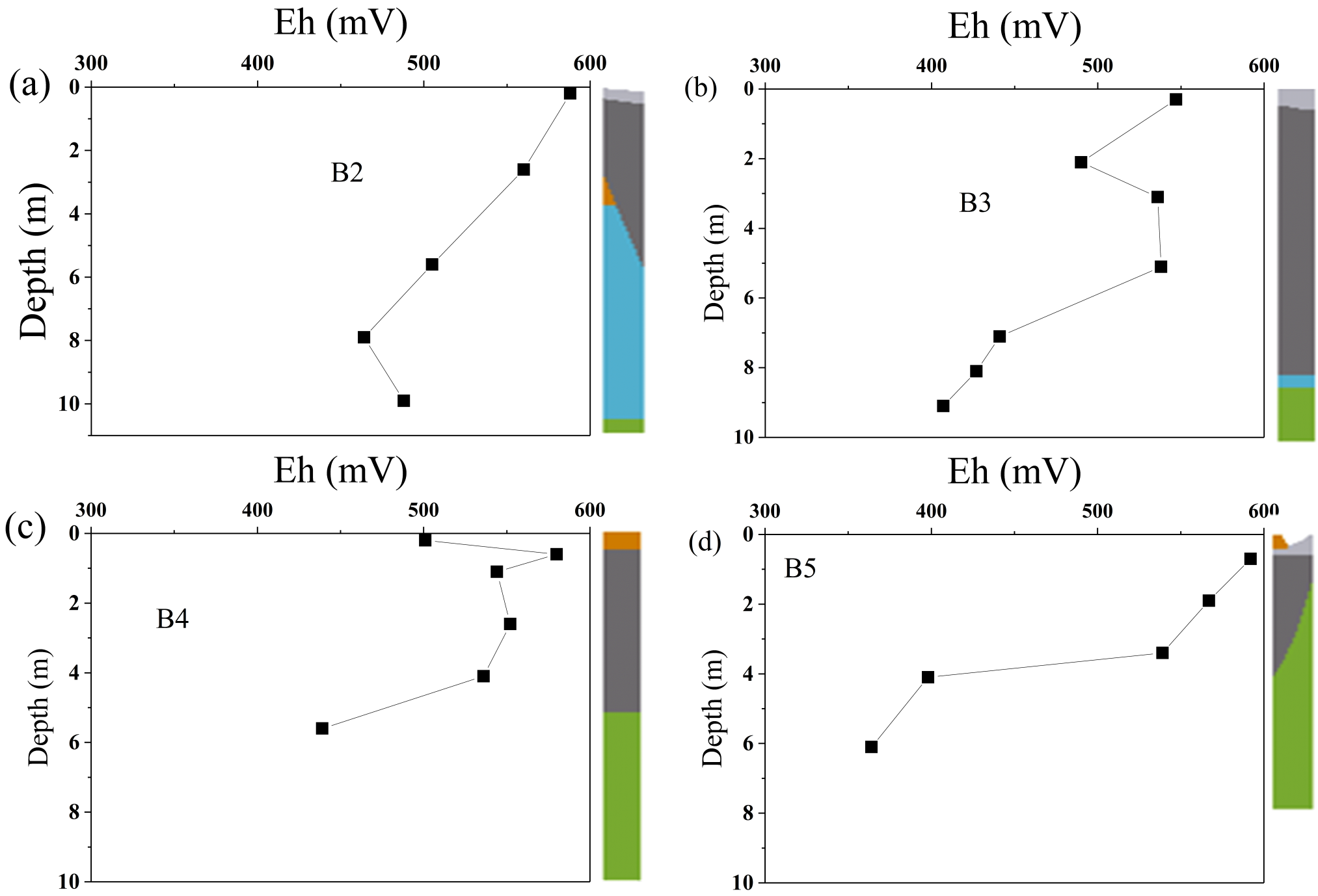
(a)
Eh (mV)
300
400
500
600
Depth (m)
0
2
4
6
8
10
B2
(b)
Eh (mV)
B3
(c)
Eh (mV)
B4
(d)
Eh (mV)
B5

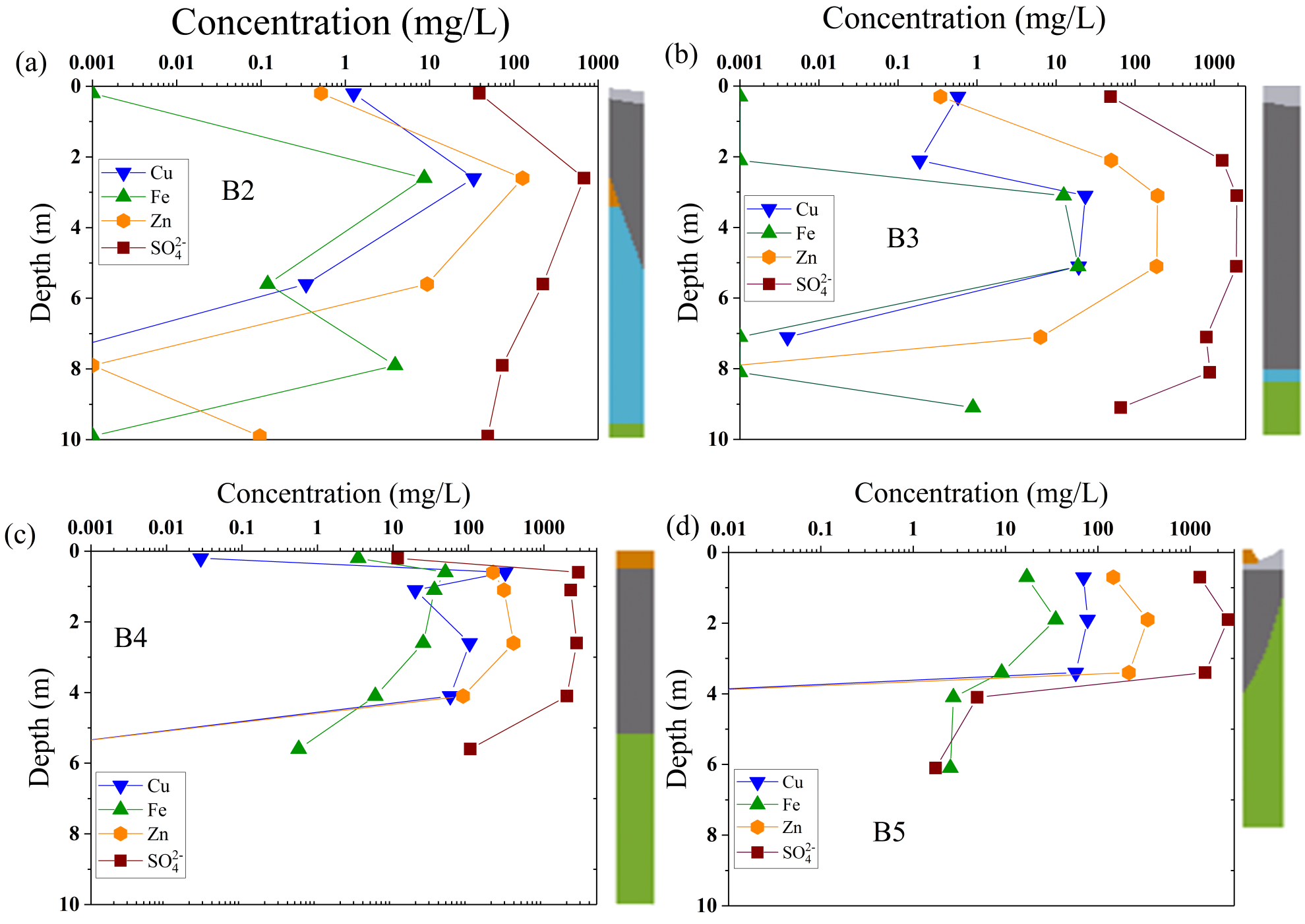
(a)
Concentration (mg/L)
0.001
0.01
0.1
1
10
100
1000
Depth (m)
0
2
4
6
8
10
Cu
Fe
Zn
SO_4^{2-}
B2
(b)
Concentration (mg/L)
B3
(c)
Concentration (mg/L)
B4
(d)
Concentration (mg/L)
B5

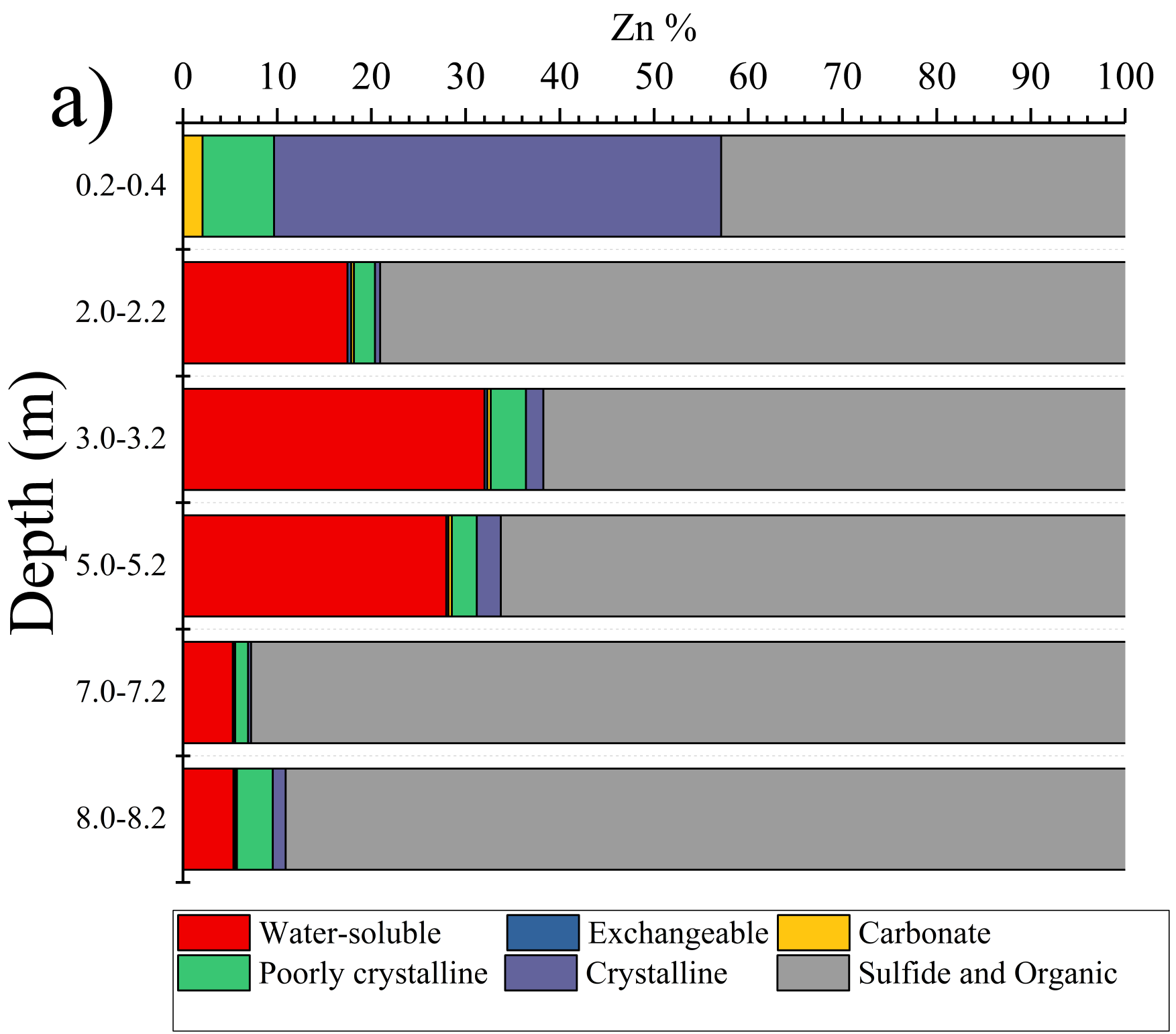
a)
Zn %
0
10
20
30
40
50
60
70
80
90
100
Depth (m)
0.2-0.4
2.0-2.2
3.0-3.2
5.0-5.2
7.0-7.2
8.0-8.2
Water-soluble
Exchangeable
Carbonate
Poorly crystalline
Crystalline
Sulfide and Organic

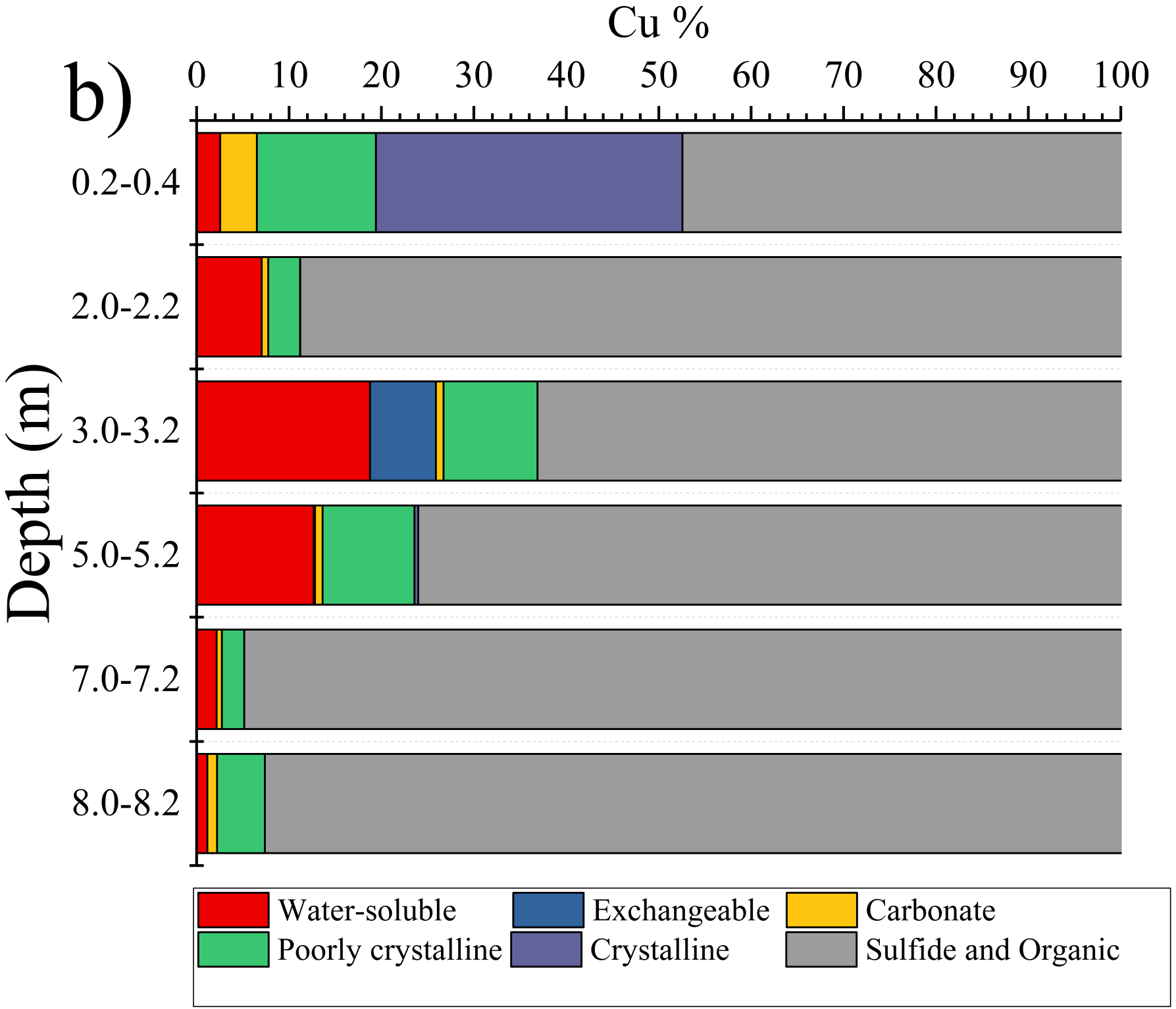
b)
Cu %
0
10
20
30
40
50
60
70
80
90
100
Depth (m)
0.2-0.4
2.0-2.2
3.0-3.2
5.0-5.2
7.0-7.2
8.0-8.2
Water-soluble
Exchangeable
Carbonate
Poorly crystalline
Crystalline
Sulfide and Organic

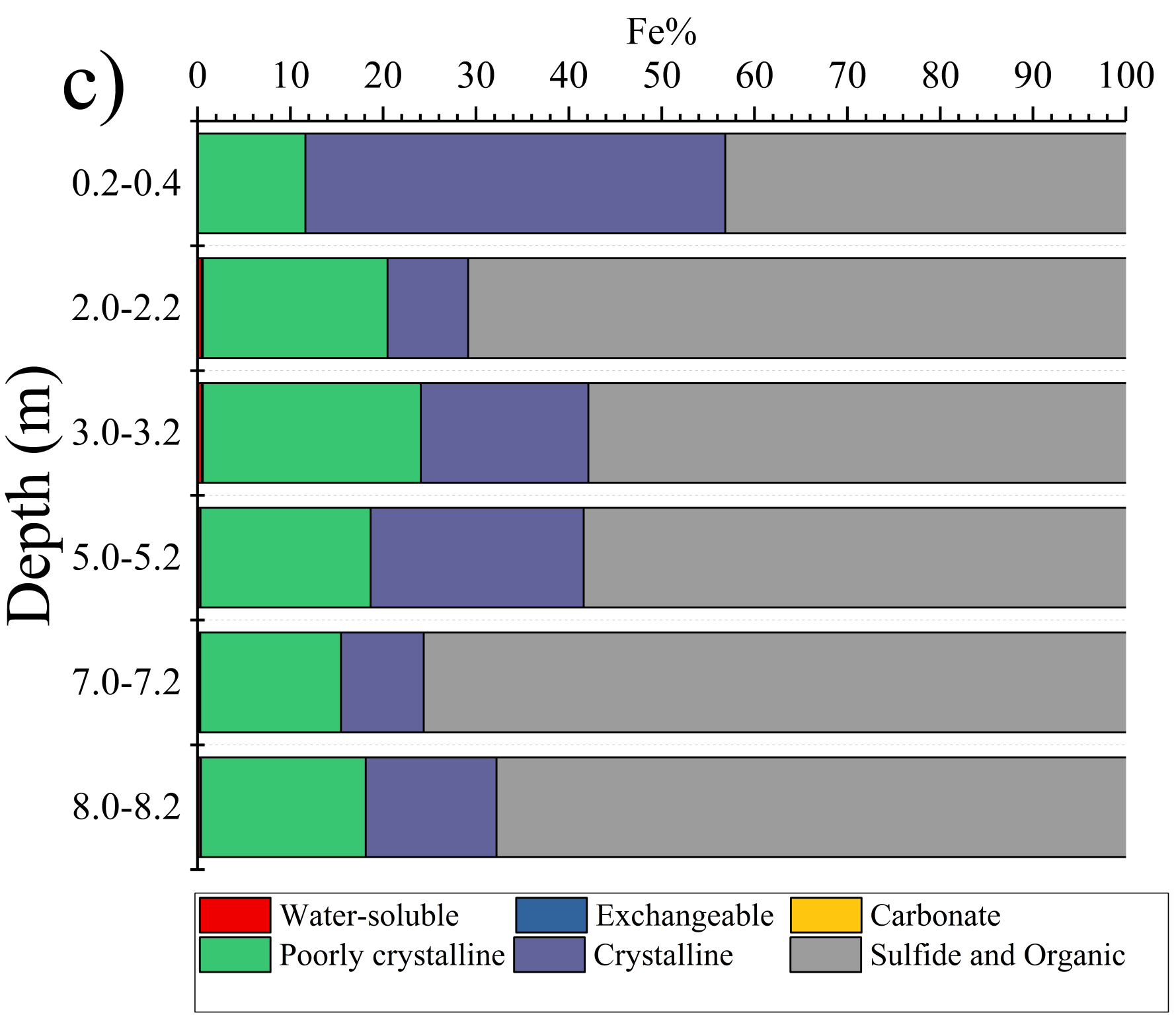
c)
Fe%
0
10
20
30
40
50
60
70
80
90
100
Depth (m)
0.2-0.4
2.0-2.2
3.0-3.2
5.0-5.2
7.0-7.2
8.0-8.2
Water-soluble
Exchangeable
Carbonate
Poorly crystalline
Crystalline
Sulfide and Organic

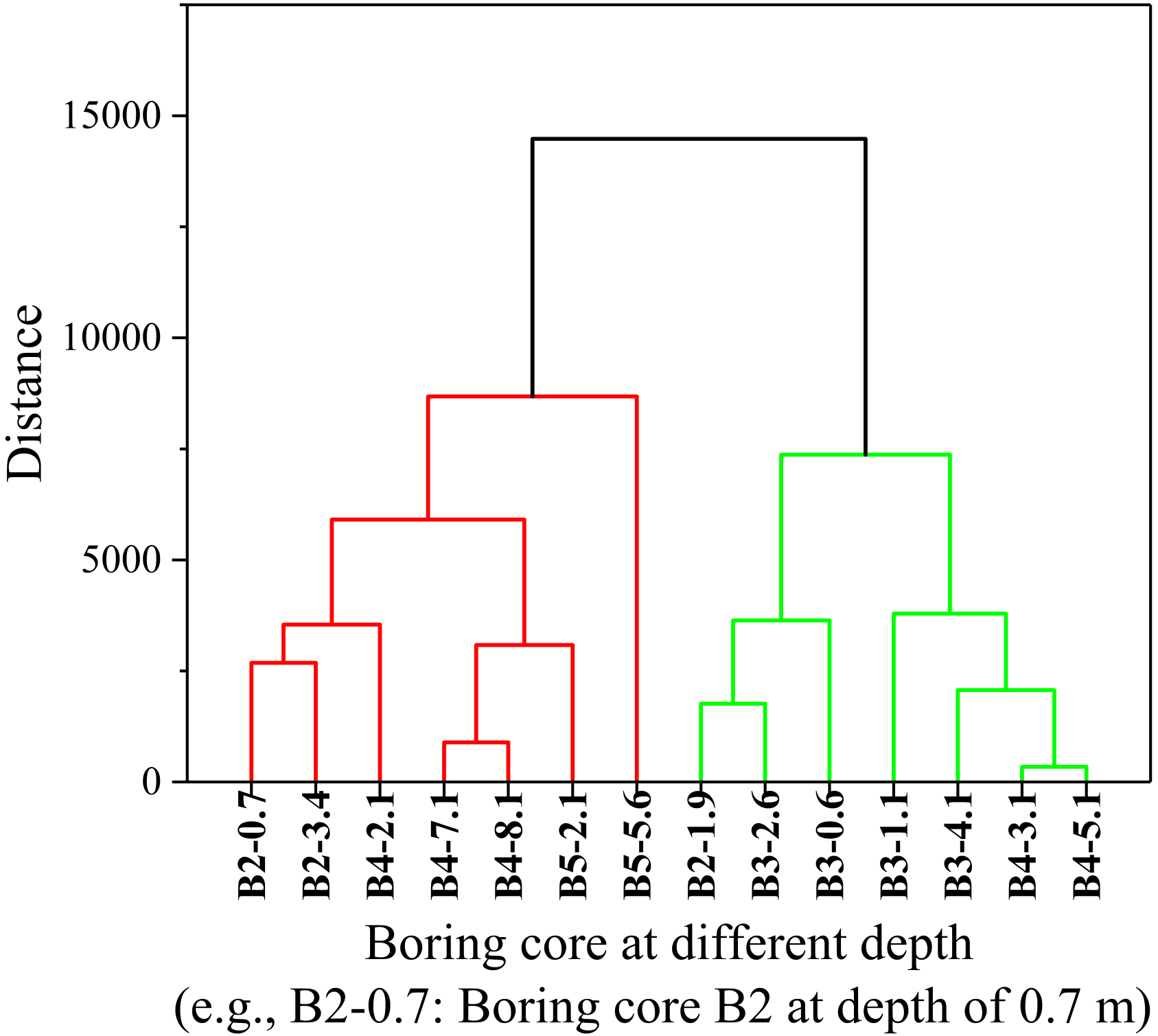
15000
10000
5000
0
Distance
B2-0.7
B2-3.4
B4-2.1
B4-7.1
B4-8.1
B5-2.1
B5-5.6
B2-1.9
B3-2.6
B3-0.6
B3-1.1
B3-4.1
B4-3.1
B4-5.1
Boring core at different depth
(e.g., B2-0.7: Boring core B2 at depth of 0.7 m)